Design of Deep-UV Nanowire LED with Al_2O_3 Quantum Dots and Step-Graded n-type AlInGaN Electron Blocking Layer for High Quantum Efficiency

Samadrita Das
Department of Electronics and Communication Engineering
National Institute of Technology
Silchar, Assam, India
samadrita_rs@ece.nits.ac.in

Trupti Ranjan Lenka
Department of Electronics and Communication Engineering
National Institute of Technology
Silchar, Assam, India
trlenka@ieee.org

Fazal Ahmed Talukdar
Department of Electronics and Communication Engineering
National Institute of Technology
Silchar, Assam, India
fazal@ece.nits.ac.in

Hieu Pham Trung Nguyen
Department of Electrical and Computer Engineering
New Jersey Institute of Technology,
Newark, USA
hieu.p.nguyen@njit.edu

IECON 2023- 49th Annual Conference of the IEEE Industrial Electronics Society | 979-8-3503-3182-0/23/$31.00 ©2023 IEEE | DOI: 10.1109/IECON51785.2023.10312022

***Abstract*— In this paper, we have proposed a novel deep ultra-violet (DUV) AlGaN/GaN nanowire light-emitting diode (LED) with a step-graded n-type AlInGaN electron blocking layer (EBL) instead of a conventional p-type AlGaN EBL. The nanowire is designed with Al_2O_3 quantum dots (QDs) deposited all over the substrate. The proposed nanowire is designed for a ~265 nm wavelength emission without affecting the hole injection efficiency. Due to enhanced carrier transport in the step-graded n-type EBL structure, there occurs reduced electron leakage into the p-region, superior hole activation and hole injection, improved output power and internal quantum efficiency (IQE). Moreover, this specially designed EBL reduces the quantum confined stark effect in the active region, ultimately enhancing the carrier wave functions overlap. The device structure is simulated using Atlas technology computer-aided design (TCAD). The efficiency is improved from ~36.48% to ~49.46% while switching from conventional p-type EBL to step-graded n-type EBL. Furthermore, our proposed structure exhibits 1.61% efficiency droop, which is significantly ~4.8 times lower as compared to the regular structure.**

Keywords*— Electron blocking layer (EBL); internal quantum efficiency (IQE); light-emitting diode (LED); multi-quantum well (MQW).

I. Introduction

DUE to the wide band-gap, aluminium gallium nitride (AlGaN) based deep ultra-violet (DUV) light-emitting diodes (LED) are capable of replacing the existing incandescent UV light sources for a wide range of applications, such as water purification, pharmaceutical applications, and disinfection [1]–[4]. III-nitrides like gallium nitride (GaN), indium nitride (InN), aluminium nitride (AlN) and their alloys have energies ranging from 0.7 eV (InN) through 3.4 eV (GaN) to 6.2 eV (AlN), making them uniquely suitable for visible and ultra-violet LEDs. Across the entire UV-A, UV-B, and UV-C spectral range, UV LEDs offer significantly decreased power consumption, low cost, and reduced space [5]–[8].

Optical power and internal quantum efficiency (IQE) are considered to be the critical parameters, which need further improvement so that high-power LEDs can penetrate into the consumer industry of lighting [9][10]. However it gets hindered by the electron overflow into the p-GaN region and the inadequate hole supply into the active region [11][12]. Due to overflow of electrons, the compactness of carriers inside the wells will be minimised which will lead to poor radiative recombination. Therefore to restrict this overflow, a p-type electron blocking layer (EBL) is inserted between the active region and p-GaN layers. The electrons are thus confined within the multi-quantum well (MQW) because of the huge potential barrier created by AlGaN layer, resulting in a low electron overflow. Because of the large defect density and dislocation in the active region, it is still difficult to obtain efficient p-type conduction in large Al content EBL [13]–[16]. This occurs due to various reasons related with magnesium (Mg)-dopants including tremendously large activation energy (till ~600 meV), little tendency to get soluble and self-compensation while forming point defects [17][18]. Because of in-effective Mg-doping, a very poor hole concentration occurs in this Al rich EBL [19]–[21]. Also when the potential barrier height difference is large, it obstructs the hole transportation into the MQWs leading to insufficient hole supply taking part in the radiative recombination with electrons [22]. Therefore in an attempt to minimize electron overflow without compromising the hole injection, a novel LED nanowire structure has been proposed in this paper using step-graded n-type AlInGaN EBL inserted between the active region and n-AlGaN cladding layer. This EBL consists of silicon (Si)-doped AlInGaN permitting effective cooling of hot electrons before they inject into the active region and thus there is a less overflow of electrons. The proposed nanowire LED is surrounded by Al_2O_3 nanoparticles with very low radius which results in low self-heating of the device. In our proposed device, due to step-graded EBL structure, the kinetic energy and electron velocity inserting the active region decrease which in turn reduce the electron mean free path and improve the electron confinement in the EBL [23]. This paper is structured as follows: Section II is dedicated to a brief description of the simulation methodology, presentation of the device structure and parameters. Section III is focused on the presentation and discussion of the obtained results, and, finally, the conclusions are given in the last section.

II. Device Structure And Parameters

Firstly, in order to validate our device model, we have examined the conventional AlGaN deep UV LED formed on a c-plane AlN template with ~284 nm emission wavelength as our reference device and denoted as LED_1. This work was studied and experimentally presented by Yan et al [24]. LED_1 comprises of 3 μm n-$Al_{0.6}Ga_{0.4}N$ layer (Si doping: 5×10^{18} cm^{-3}), followed by an active region, p-$Al_{0.65}Ga_{0.35}N$ EBL (20 nm, Mg doping: 2×10^{19} cm^{-3}) and then capped by a 50 nm p-$Al_{0.5}Ga_{0.5}N$ hole injection layer (Mg doping: 2×10^{19} cm^{-3}), and on the top a 80 nm p-GaN contact layer (Mg doping: 1×10^{20} cm^{-3}). The active region comprises of five intrinsic $Al_{0.4}Ga_{0.6}N$ quantum wells (QWs of 3 nm) stuffed between six intrinsic $Al_{0.5}Ga_{0.5}N$ quantum barriers (QBs of 12 nm). As illustrated in Fig. 1, the proposed device (LED_2) is designed as a nanowire and has the similar layers as LED_1 except that the uniform p-type AlGaN EBL is now replaced by step-graded n-type AlInGaN EBL prior to the active region. Also LED_2 nanowire is designed with Al_2O_3 quantum dots (QDs) deposited all over the substrate. In this nanowire sapphire is used as the substrate due to the benefit of high heat conductivity and allowing for vertical conduction geometry. During the simulation the radius of the nanoparticles is taken as 10 nm. The LED chip has an overall area of 300 μm×300 μm which is operated under a temperature of 300 K and the internal absorption loss is assumed as 2000 m^{-1}.

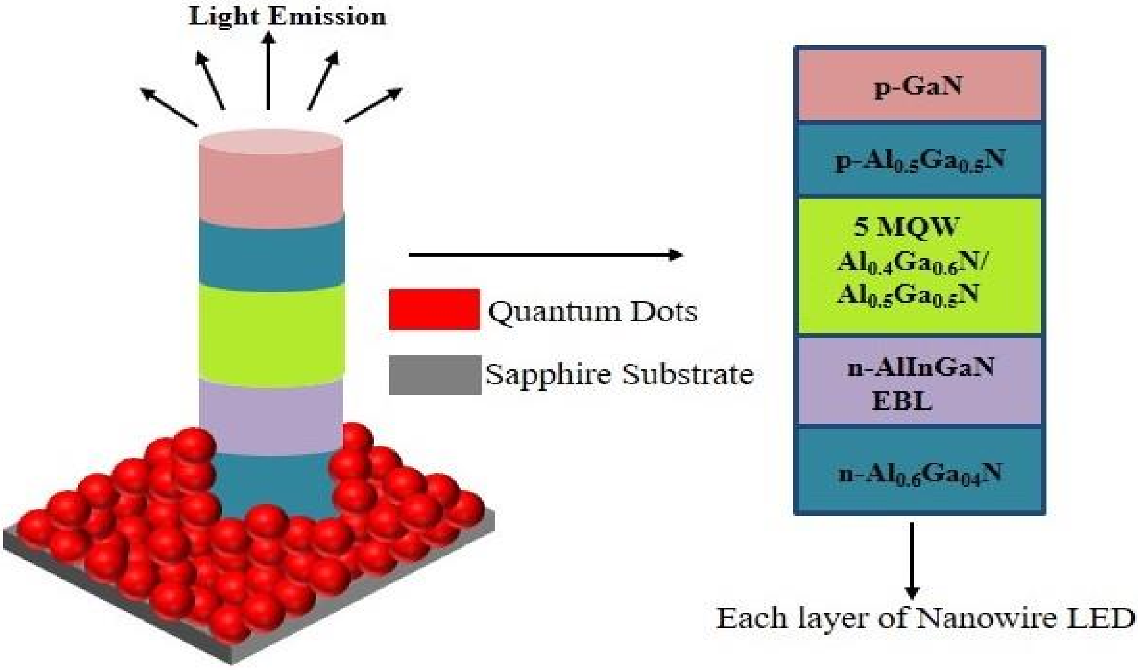

Fig. 1. Schematic diagram of the proposed nanowire LED (LED_2) with n-type EBL and Al_2O_3 nanoparticles deposited over the substrate.

The benefit of n-type EBL consisting of AlInGaN step-graded layers is the effective cooling of hot electrons before injecting in the active region and thus minimizing overflow of electrons. Also due to the absence of any potential barrier, effective injection of holes can be achieved into the active region. Because of minimized reduced barrier to hole injection, a lower turn-on voltage for n-type EBL is obtained. The EBL of LED_2 is divided into five layers of $Al_xIn_yGa_zN$; each has a thickness of 4 nm. This layer is uniformly step-graded in such a way that the constituent values of x, y, z is (0.8, 0.03, 0.17), followed by step-wise reduction of Al composition by 10% and 10% increase of gallium composition in each layer (0.7, 0.03, 0.27 for next layer) and so on up to five consecutive divisions till (0.4, 0.03, 0.57) in the last layer.

The band-gap of GaN and AlN are taken as 3.42 eV and 6.2 eV, respectively [25]. The Auger recombination, radiative recombination, SRH recombination coefficient, and light extraction efficiency are taken as 2.88×10^{-30} cm^6/s, 2.13×10^{-11} cm^3/s, $6.67\times10^7/s$, and 15%, respectively [26]. Also, the Mg activation energy is scaled linearly from 170 meV to 510 meV for p-$Al_xGa_{1-x}N$ alloy. The electron and hole mobilities are estimated by Cauchy-Thomas approximation and band energy diagrams are measured by using 6×6 k.p model [26].

III. Results And Discussion

The device model and parameters which are numerically implemented in our work are optimized using the experimentally obtained data of reference structure i.e., LED_1.

To investigate the performance of the proposed structure, the electroluminescence (EL) spectra of the designed LEDs are displayed in Fig. 2 at an injection current of 40 mA. The light intensity of LED_2 (peak wavelength 260.9 nm) is stronger as compared to LED_1 (peak wavelength 262.8 nm). The presence of a shoulder at ~264.5 nm other than the main peak at ~262.8 nm for LED_1 is due to significant electron overflow and the resulting parasitic emission from p-AlGaN layer. Due to decrease in peak wavelength of LED_2, a very minute blue-shift is observed which is apparently assigned to the minimization of quantum-confined stark effect (QCSE) in our final structure. From Fig 2(b), LED_2 shows a prominent blue-shift when compared with the conventional LED_1. The blue shift due to the band-filling effect and screening effect causes the wavelength to initially shift towards a lower value as the current increases. But when the current continues to rise, the wavelength moves to a longer value known as red shift. This is a result of the thermal effect created by parasitic resistances at the wavelength point where there is a change from blue shift to red shift, as seen by the dashed line in Fig 2(b). In order to understand the underlying mechanism, the energy band diagram and the quasi-Fermi level of the simulated structures are analysed at 40 mA current in Figs. 3(a) and 3(b). The effective conduction band barrier height CBBH (Φ_C) at each barrier (n) and EBL (Φ_{EBL}) of LED_2 is comparatively higher than LED_1 as listed in Table 1. The higher and progressively improved Φ_C in LED_2 constructively confines the electrons in the active region and resists the electron overflow into the p-region. From Fig. 3(a) the p-type EBL generates an energy barrier height of 169.4 meV for holes. On the contrary, in Fig. 3(b), the n-type AlInGaN builds up an energy barrier of 90 meV for electrons before they enter the MQWs active region. Meanwhile, the

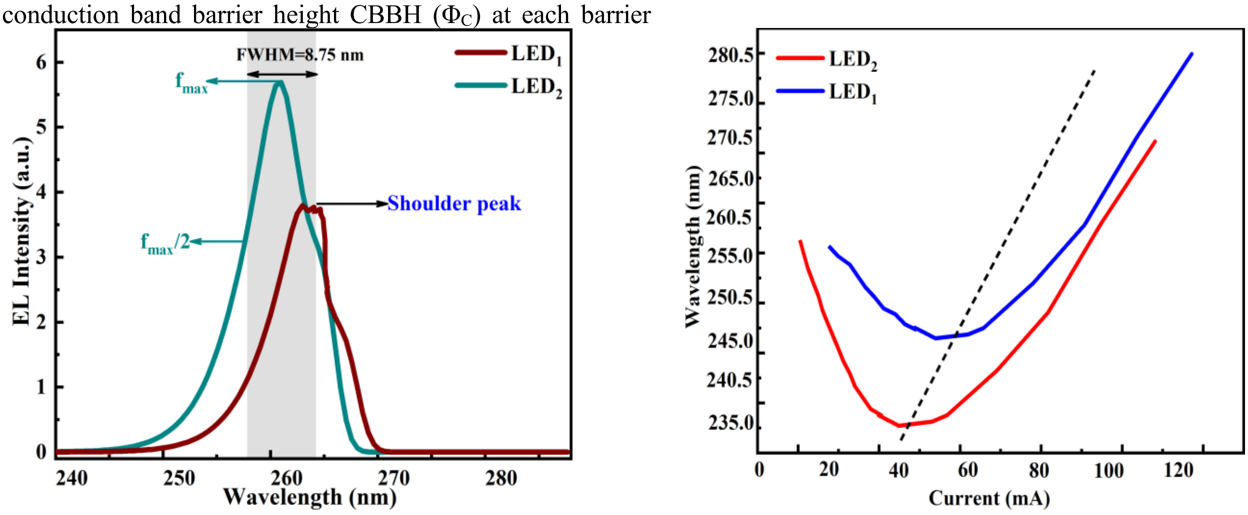

(a) (b)

Fig. 2. (a) Electroluminescence (EL) intensity of LED_1 and LED_2 at an injection current of 40 mA, (b) Emission wavelengths as a function of injection current for LED_1 and LED_2.

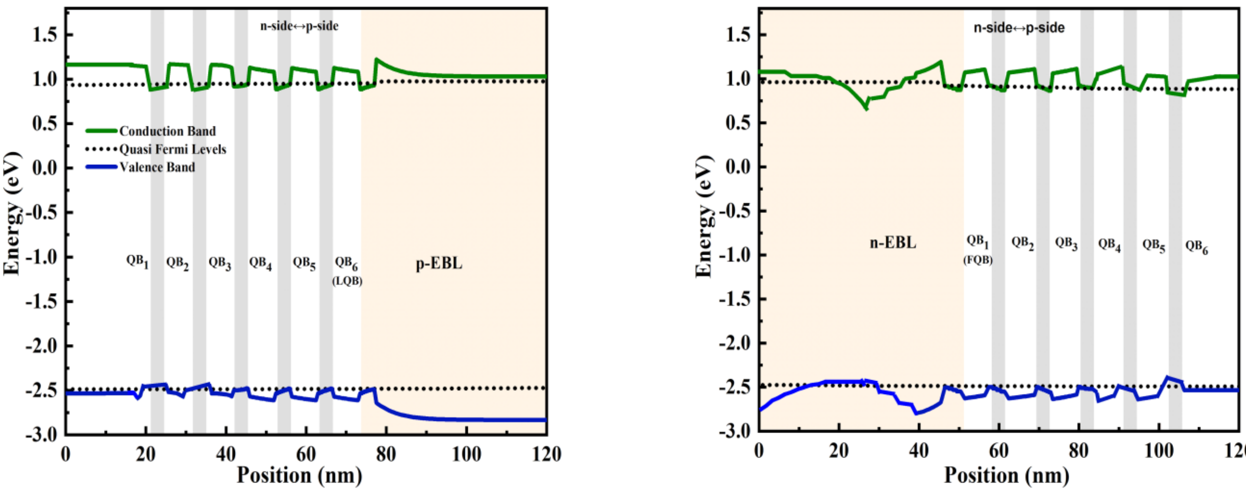

(a) (b)

Fig. 3. Energy band profile of (a) the conventional LED (LED_1) and of (b) the proposed LED (LED_2) at 40 mA.

n-EBL presents no blocking effect on the hole transport path into the QWs due to the absence of energy barrier. This leads to the reduction of non-radiative recombination in p-region and improves hole injection into the active region.

TABLE I. EFFECTIVE CBBH (Φ_{EN}), VBBH (Φ_{HN}) OF QBS AND EBL (Φ_{EBL}) FOR LED_1 AND LED_2 (IN MEV)

CBBH	LED_1	LED_2	VBBH	LED_1	LED_2
Φ_{e2}	107.8	197.1	Φ_{h2}	72.9	75.9
Φ_{e3}	159.1	203.7	Φ_{h3}	76.8	80.8
Φ_{e4}	180.4	312.7	Φ_{h4}	72.2	84.6
Φ_{e5}	176.6	367	Φ_{h5}	81.6	86.2
Φ_{e6}	174.7	343.9	Φ_{h6}	80.3	107.1
Φ_{EBL}	255.46	368.04			

In LED_2 electrons need to overcome a higher CBBH to reach the p-layer. Because of this, non-radiative recombination of leaked electrons within the holes in the p-side is lowered and availability of holes to be injected towards the active region is more. Consequently a better radiative recombination rate is observed in LED_2, due to stronger carrier concentration, as displayed in Fig. 4. For clear visualization, the position of values in the x-axis is slightly shifted for the two samples. The electron-hole pair recombination for LED_2 is enormously improved by 93.3% than LED_1 (for reference, third QW is considered).

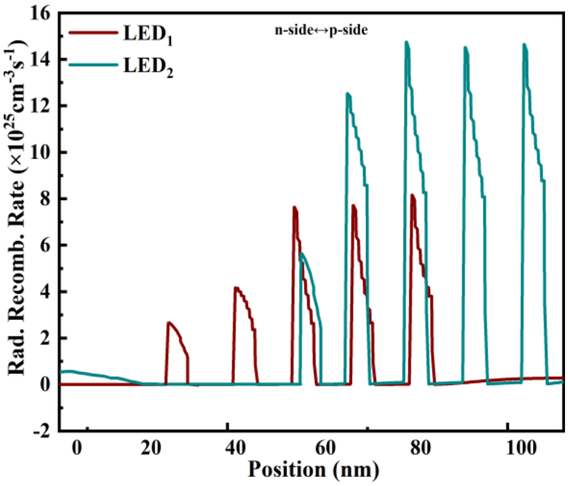

Fig. 4. Radiative recombination rate of both LED_1 and LED_2 at 40 mA.

To understand the carrier transport improvement in the proposed structure (LED_2) we have studied their corresponding IQE and output power performance, as presented in Fig. 5 and 6 respectively. It is apparent that IQE is significantly higher for LED_2 with step-graded n-type EBL by 35.58% at a current injection of 40 mA. This indicates the detrimental impact of p-type EBL on hole injection. Interestingly, the efficiency droop defined as $(\eta_{peak}-\eta_{40\ mA})/\eta_{peak}$, is severely decreased up to ~1.61% in LED_2, while LED_1 exhibits ~9.42% droop at 40 mA current. This is due to the enhanced carrier transportation and confinement of carriers in the active region of LED_2.

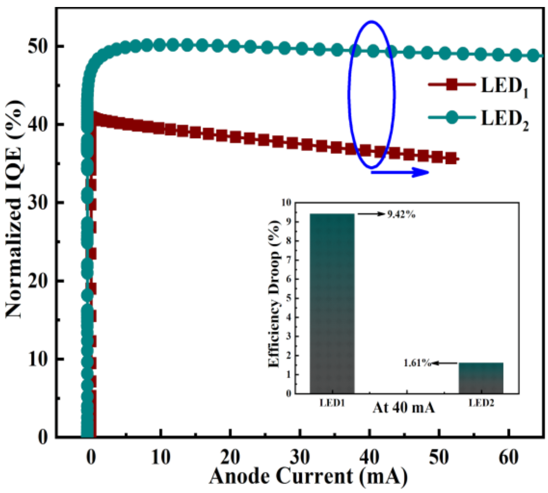

Fig. 5. IQE as a function of injected current in both LED_1 and LED_2. Inset: Efficiency droop for each LED at 40 mA.

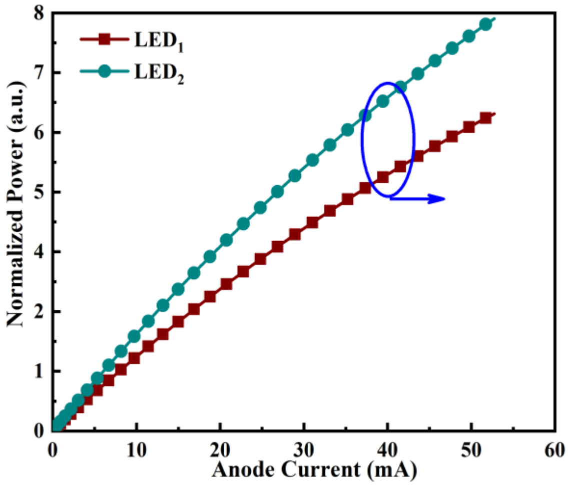

Fig. 6. Output power of both LED_1 and LED_2 as a function of injection current.

The amelioration in the IQE and decrease in droop in LED_2 are attributed to the improved radiative recombination and reduced carrier leakage, owing to superior carrier confinement. This is provided by the step-graded n-type EBL. As shown in Fig. 7, the turn-on voltage of the two structures is nearly the same. However, it is inevitable that LED_2 exhibits a slightly higher operating bias voltage at 40 mA than LED_1 due to the presence of step graded n-type AlInGaN EBL.

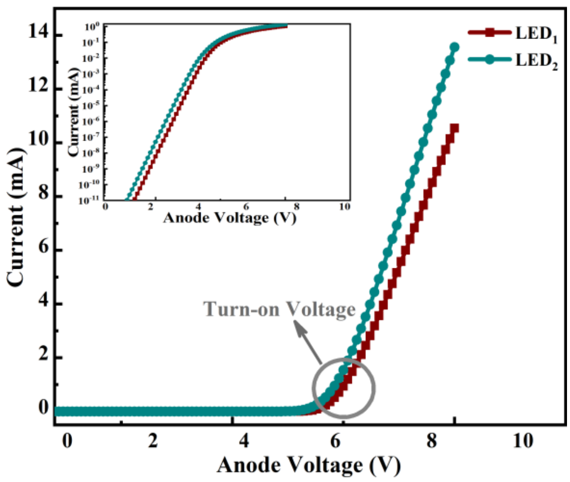

Fig. 7. I-V behavior of both LED_1 and LED_2 in linear scales; Inset: Re-plotting of the I-V curves in a semi-log scale.

IV. Conclusion

In conclusion, we have explored the impact of EBL on the output performance of AlGaN UV LEDs. From the achieved simulation results, it is evident that step-graded n-type AlInGaN EBL has better advantages compared to conventional p-type AlGaN EBL. LED_2 is superior to LED_1 as it reduces electron overflow without compromising hole transport and hole injection into the active region, thereby having a better balance between hole and electron injection in the active region. Step-graded promotes the hole injection by forming negative sheet polarization charges and improves the spatial overlap of the electron-hole wave function. A significant improvement in both IQE (by 23.51%) and power (by 71.48%) of LED_2 is measured compared to LED_1. Furthermore LED_2 is observed to have a minimal efficiency droop of 1.172% and lower electrostatic field. In the future, extended device performance is expected by optimizing the p-type doping which will further improve the light extraction efficiency along with minimized efficiency droop. While this work is preliminary, continued refinement of this technology platform offers exciting new approaches to improved performance and manufacturing of solid-state lighting systems.

ACKNOWLEDGMENT

This work is the outcome of DST-SERB, Govt. of India which is duly acknowledged for kind support.

REFERENCES

[1] K. Davitt, Y.-K. Song, W. R. Patterson III, A. V. Nurmikko, M. Gherasimova, J. Han, Y.-L. Pan, and R. K. Chang, "290 and 340 nm UV LED arrays for fluorescence detection from single airborne particles," Opt. Express, vol. 13, no. 23, p. 9548, 2005, doi: 10.1364/opex.13.009548.

[2] L. Kemény, Z. Csoma, E. Bagdi, A. H. Banham, L. Krenács, and A. Koreck, "Targeted phototherapy of plaque-type psoriasis using ultraviolet B-light-emitting diodes," Br. J. Dermatol., vol. 163, no. 1, pp. 167–173, 2010, doi: 10.1111/j.1365-2133.2010.09763.x.

[3] P. J. Parbrook and T. Wang, "Light emitting and laser diodes in the ultraviolet," IEEE J. Sel. Top. Quantum Electron., vol. 17, no. 5, pp. 1402–1411, 2011, doi: 10.1109/JSTQE.2011.2126563.

[4] A. Khan, K. Balakrishnan, and T. Katona, "Ultraviolet light-emitting diodes based on group three nitrides," Nat. Photonics, vol. 2, no. 2, pp. 77–84, 2008, doi: 10.1038/nphoton.2007.293.

[5] H. Hirayama, N. Maeda, S. Fujikawa, S. Toyoda, and N. Kamata, "Recent progress and future prospects of AlGaN- diodes," Jpn. J. Appl. Phys., vol. 53, no. 10, p. 100209, 2014.

[6] H. Sun and T. D. Moustakas, "UV emitters based on an AlGaN p-n junction in the form of graded-index separate confinement heterostructure," Appl. Phys. Express, vol. 7, no. 1, pp. 1–4, 2014, doi: 10.7567/APEX.7.012104.

[7] Y. Kashima, N. Maeda, E. Matsuura, M. Jo, T. Iwai, T. Morita, M. Kokubo, T. Tashiro, R. Kamimura, Y. Osada, H. Takagi, and H. Hirayama, "High external quantum efficiency (10%) AlGaN-based deep-ultraviolet light-emitting diodes achieved by using highly reflective photonic crystal on p-AlGaN contact layer," Appl. Phys. Express, vol. 11, no. 1, 2018, doi: 10.7567/APEX.11.012101.

[8] M. Jo, N. Maeda, and H. Hirayama, "Enhanced light extraction in 260nm light-emitting diode with a highly transparent p-AlGaN layer," Appl. Phys. Express, vol. 9, no. 1, pp. 7–10, 2016, doi: 10.7567/APEX.9.012102.

[9] M. H. Crawford, "LEDs for solid-state lighting: Performance challenges and recent advances," IEEE J. Sel. Top. Quantum Electron., vol. 15, no. 4, pp. 1028–1040, 2009, doi: 10.1109/JSTQE.2009.2013476.

[10] N. Tansu, H. Zhao, G. Liu, X. H. Li, J. Zhang, H. Tong, and Y. K. Ee, "III-nitride photonics," IEEE Photonics J., vol. 2, no. 2, pp. 241–248, 2010, doi: 10.1109/JPHOT.2010.2045887.

[11] D. S. Shin, D. P. Han, J. Y. Oh, and J. I. Shim, "Study of droop phenomena in InGaN-based blue and green light-emitting diodes by temperature-dependent electroluminescence," Appl. Phys. Lett., vol. 100, no. 15, 2012, doi: 10.1063/1.3703313.

[12] M. H. Kim, M. F. Schubert, Q. Dai, J. K. Kim, E. F. Schubert, J. Piprek, and Y. Park, "Origin of efficiency droop in GaN-based light-emitting diodes," Appl. Phys. Lett., vol. 91, no. 18, pp. 1–4, 2007, doi: 10.1063/1.2800290.

[13] T. D. Moustakas, "Ultraviolet optoelectronic devices based on AlGaN alloys grown by molecular beam epitaxy," MRS Commun., vol. 6, no. 3, pp. 247–269, 2016, doi: 10.1557/mrc.2016.26.

[14] S. I. Inoue, N. Tamari, and M. Taniguchi, "150 mW deep-ultraviolet light-emitting diodes with large-area AlN nanophotonic light-extraction structure emitting at 265 nm," Appl. Phys. Lett., vol. 110, no. 14, 2017, doi: 10.1063/1.4978855.

[15] J. S. Speck, "Role of threading dislocations in the physical properties of GaN and its alloys," Mater. Sci. Forum, vol. 353–356, pp. 769–778, 2001, doi: 10.4028/www.scientific.net/msf.353-356.769.

[16] M. H. Chang, D. Das, P. V. Varde, and M. Pecht, "Light emitting diodes reliability review," Microelectron. Reliab., vol. 52, no. 5, pp. 762–782, 2012, doi: 10.1016/j.microrel.2011.07.063.

[17] C. Stampfl and C. G. Van de Walle, "Theoretical investigation of native defects, impurities, and complexes in aluminum nitride," Phys. Rev. B - Condens. Matter Mater. Phys., vol. 65, no. 15, pp. 1552121–15521210, 2002, doi: 10.1103/PhysRevB.65.155212.

[18] A. You, M. A. Y. Be, and I. In, "Doping of," vol. 459, no. November 1997, 2018.

[19] Y. H. Liang and E. Towe, "Progress in efficient doping of high aluminum-containing group III-nitrides," Appl. Phys. Rev., vol. 5, no. 1, 2018, doi: 10.1063/1.5009349.

[20] K. Ebata, J. Nishinaka, Y. Taniyasu, and K. Kumakura, "High hole concentration in Mg-doped AlN/AlGaN superlattices with high Al content," Jpn. J. Appl. Phys., vol. 57, no. 4, pp. 4–7, 2018, doi: 10.7567/JJAP.57.04FH09.

[21] Y. Chen, H. Wu, E. Han, G. Yue, Z. Chen, Z. Wu, G. Wang, and H. Jiang, "High hole concentration in p-type AlGaN by indium-surfactant-assisted Mg-delta doping," Appl. Phys. Lett., vol. 106, no. 16, 2015, doi: 10.1063/1.4919005.

[22] H. Hirayama, Y. Tsukada, T. Maeda, and N. Kamata, "Marked enhancement in the efficiency of deep-ultraviolet AlGaN light-emitting diodes by using a multiquantum-barrier electron blocking layer," Appl. Phys. Express, vol. 3, no. 3, pp. 3–6, 2010, doi: 10.1143/APEX.3.031002.

[23] S. H. Han, D. Y. Lee, S. J. Lee, C. Y. Cho, M. K. Kwon, S. P. Lee, D. Y. Noh, D. J. Kim, Y. C. Kim, and S. J. Park, "Effect of electron blocking layer on efficiency droop in InGaN/GaN multiple quantum well light-emitting diodes," Appl. Phys. Lett., vol. 94, no. 23, pp. 1–5, 2009, doi: 10.1063/1.3153508.

[24] Y. Li, S. Chen, W. Tian, Z. Wu, Y. Fang, J. Dai, and C. Chen, "Advantages of AlGaN-based 310-nm UV light-emitting diodes with Al content graded AlGaN electron blocking layers," IEEE Photonics J., vol. 5, no. 4, p. 8200309, 2013, doi: 10.1109/JPHOT.2013.2271718.

[25] S. Das, T. R. Lenka, F. A. Talukdar, R. T. Velpula, B. Jain, H. P. T. Nguyen, and G. Crupi, "Effects of polarized-induced doping and graded composition in an advanced multiple quantum well InGaN/GaN UV-LED for enhanced light technology," Eng. Res. Express, 2022, doi: 10.1088/2631-8695/ac4fb1.

[26] S. Clara, "Silvaco User's Manual DEVICE SIMULATION SOFTWARE," no. October, 2004, [Online]. Available: www.silvaco.com.